npg

ORIGINAL ARTICLE

Genomic collinearity and the genetic architecture of floral differences between the homoploid hybrid species *Iris nelsonii* and one of its progenitors, *Iris hexagona*

SJ Taylor, LD Rojas, SW Ho and NH Martin

Hybrid speciation represents a relatively rapid form of diversification. Early models of homoploid hybrid speciation suggested that reproductive isolation between the hybrid species and progenitors primarily resulted from karyotypic differences between the species. However, genic incompatibilities and ecological divergence may also be responsible for isolation. *Iris nelsonii* is an example of a homoploid hybrid species that is likely isolated from its progenitors primarily by strong prezygotic isolation, including habitat divergence, floral isolation and post-pollination prezygotic barriers. Here, we used linkage mapping and quantitative trait locus (QTL) mapping approaches to investigate genomic collinearity and the genetic architecture of floral differences between *I. nelsonii* and one of its progenitor species *I. hexagona*. The linkage map produced from this cross is highly collinear with another linkage map produced between *I. fulva* and *I. brevicaulis* (the two other species shown to have contributed to the genomic makeup of *I. nelsonii*), suggesting that karyotypic differences do not contribute substantially to isolation in this homoploid hybrid species. Similar to other studies of the genetic architecture of floral characteristics, at least one QTL was found that explained > 20% variance in each color trait, while minor QTLs were detected for each morphological trait. These QTLs will serve as hypotheses for regions under selection by pollinators.
Heredity (2013) **110**, 63–70; doi:10.1038/hdy.2012.62; published online 10 October 2012

INTRODUCTION

The evolution of new, reproductively isolated species usually involves the gradual accumulation of multiple prezygotic and postzygotic reproductive isolating barriers over time (Coyne and Orr, 1989, 1997; Moyle *et al.*, 2004; Malone and Fontenot, 2008; Scopece *et al.*, 2008). An exception to this is hybrid speciation, where reproductive isolation can evolve quite quickly (James and Abbott, 2005; Mallett, 2007; Buerkle and Rieseberg, 2008). Most commonly, reproductive isolation between a hybrid species and its progenitors results from postzygotic isolation caused primarily by a change in ploidy (polyploid speciation), although a growing number of hybrid species are being detected that are reproductively isolated from their progenitor species without an increase in ploidy (homoploid hybrid species; reviewed by Rieseberg and Willis, 2007).

Reproductive isolation between new homoploid hybrid species and their progenitors may result from the rapid fixation of chromosomal rearrangements and/or genic incompatibilities in addition to ecological divergence between the hybrid taxa and their parental species (Grant, 1971; Buerkle *et al.*, 2000, Buerkle and Rieseberg, 2008). A majority of homoploid hybrid species described to date have a mosaic genome (mosaic genome hybrid speciation; Jiggins *et al.*, 2008), where genomic differences are sorted in the hybrid genome through both fertility and ecological selection (Karrenberg *et al.*, 2007). In the most well studied of these systems, chromosomal rearrangements have a substantial role in strong postzygotic isolation between several independently derived homoploid hybrid sunflower

species and their progenitors (Rieseberg *et al.*, 1995; Rieseberg, 2000; Lai *et al.*, 2005), as was predicted in earlier verbal models of homoploid hybrid speciation (Grant, 1971).

Strong reproductive isolation between the homoploid hybrid species and the progenitors may also result primarily from genic differences and ecological divergence (Jiggins *et al.*, 2008). In a few identified homoploid hybrid species (for example, *Heliconius* butterflies), the introgression of relatively few traits that confer an ecological advantage may be sufficient to cause reproductive (mainly ecological) isolation (hybrid trait speciation; Jiggins *et al.*, 2008; Salazar *et al.*, 2010). Such systems present an opportunity to investigate alternative models of hybrid speciation, especially ones in which genic incompatibilities and ecological isolation are of primary importance in reproductive isolation.

One of the 'classic examples' (Coyne and Orr, 2004) of homoploid hybrid speciation is that of the Louisiana Iris species *I. nelsonii*. Randolph (1966) first described this new species and hypothesized a homoploid hybrid origin based on cytological (Randolph *et al.*, 1961) and morphological data (Randolph, 1966). Randolph (1966) suggested that *I. nelsonii* was derived from hybridization between two widespread species of Louisiana Iris (*I. fulva* and *I. hexagona*) and possibly a third widespread species (*I. brevicaulis*). These three species are all found in southern Louisiana but occupy slightly different habitats and display divergent floral phenotypes. *I. fulva* flowers are relatively small in size, have a copper red color and have reflexed sepals. The larger *I. brevicaulis* and *I. hexagona* flowers are blue, with

Department of Biology, Texas State University-San Marcos, San Marcos, TX, USA
Correspondence: SJ Taylor, Department of Biology, Texas State University-San Marcos, 601 University Drive, San Marcos, TX 78666, USA.
E-mail: st1188@txstate.edu

prominent nectar guides and stiff sepals. *I. nelsonii* flowers are dark red in color and morphologically intermediate between *I. fulva* and *I. hexagona* for some traits, while extreme to the means of the purported progenitors for others (Randolph, 1966). The hybrid origin of *I. nelsonii* was later confirmed with allozyme (Arnold *et al.*, 1990) and nuclear (Arnold, 1993) data that suggested that a majority of the *I. nelsonii* genome was derived from *I. fulva* with contributions of loci from *I. hexagona* and *I. brevicaulis*.

When Randolph (1966) initially described *I. nelsonii*, he proposed ecological isolation as a major barrier to gene flow between *I. nelsonii* and the progenitors. Indeed, *I. nelsonii* is endemic to interconnected swamp systems in southern Louisiana and responds differently than its progenitors to abiotic habitat conditions (Taylor *et al.*, 2011). In portions of its limited range, *I. nelsonii* is sympatric with one of its progenitors, *I. hexagona*. These two species occupy similar swamp habitats and respond to abiotic habitat characteristics differently than the other species of Louisiana Iris (Taylor *et al.*, 2011). However, *I. nelsonii* is often found in understory habitats, while *I. hexagona* is found in more open habitats and seems to be limited by shade (Bennett and Grace, 1990). Additionally, as reflected by their suites of floral characters, these species are pollinated by different suites of pollinators. The large blue flowers of *I. hexagona* are primarily visited by bumblebees (Emms and Arnold, 2000), while the large red flowers of *I. nelsonii* are primarily visited by ruby-throated hummingbirds (Taylor *et al.*, 2012). Pollinator isolation, thus, has the potential to be an extremely important ecological barrier to hybridization between *I. nelsonii* and one of its progenitors, *I. hexagona*.

This classic example of homoploid hybrid speciation represents an opportunity to investigate hybrid speciation where postzygotic isolation is potentially minimal between the hybrid species and progenitors and, instead, prezygotic isolation—especially ecological isolation—is responsible for inhibiting gene flow in the system. Here, we utilize a comparative mapping approach to investigate genomic collinearity between *I. nelsonii* and its progenitors, noting that increased collinearity should be consistent with the high first-generation hybrid fertility observed between these species. Additionally, we investigate the genetic architecture of floral differences between *I. nelsonii* and *I. hexagona* to identify loci potentially under selection by pollinators and responsible for ecological isolation between these taxa.

MATERIALS AND METHODS
Mapping Population
In order to produce the mapping population used herein, pollen of a wild-collected *I. nelsonii* individual (In10—collected from Vermillion Parish, LA, USA) was dusted onto the stigmatic surface of a wild-collected *I. hexagona* individual (IhA32—collected from St Martin Parish, LA, USA) to produce F_1 hybrid offspring. Flowers from a single F_1 hybrid were self-pollinated to produce the F_2 hybrid mapping population, and ultimately several hundred F_2 hybrid seeds were produced. The F_2 seeds were planted at the University of Georgia greenhouse and monitored for germination success. Successfully germinated seeds were transplanted into six-inch Azalea pots, and repotted into 8-inch Azalea pots. All F_2, F_1, and pure-species plants were transported to the Texas State University greenhouse in 2007 where they have been maintained and transplanted annually into new 10-inch Azalea pots until the present. In all, $281 F_2$ plants were used in the genetic map construction described herein.

Map construction
DNA was extracted from IhA32, In10, the F_1 and the 281 F_2 plants using a modified cetyltrimethyl ammonium bromide DNA extraction protocol. A total of 282 microsatellite primers (developed by Tang *et al.* (2009) for *I. fulva* and

I. brevicaulis map production) were screened for utility in the *I. nelsonii* × *I. hexagona* F_2 mapping population. Of those, 137 markers were both polymorphic and reliably scored in the mapping population. The marker names reported here are the same as those reported for linkage maps previously constructed using *I. brevicaulis* × *I. fulva* reciprocal backcross populations (Tang *et al.*, 2010). PCR reactions (modified from Tang *et al.*, 2009) were performed in 10 µl reaction volumes that included 1x PCR buffer, 2.5 mM MgCl₂, 0.3 mM of each deoxyribonucleotide triphosphate, 4 pmol fluorescently labeled forward primer (either 6-FAM/HEX/TAMRA dye), 4 pmol reverse primer, 0.5 units *GoTaq* Flexi DNA Polymerase (Promega Corporation, Madison, WI, USA), and ∼10 ng of genomic DNA. Loci were amplified using touchdown PCR (Don *et al.*, 1991) to minimize nonspecific amplification. Thermocycling conditions were as follows: initial denaturation was at 94 °C for 1 minute followed by six cycles of: 94 °C for 30 s, 64 °C (decreasing in 1 °C increments each cycle to 58 °C) for 30 s, 72 °C for 30 s, then 33 cycles of: 94 °C for 20 s, 58 ºC for 20 s, 72 °C for 30 s with a final extension period of 72 °C for 15 min (Tang *et al.*, 2009). Fragments were multiplexed when possible (when fluorescent labels and/or allele sizes allowed for multiplexing) and run on an ABI 3700xl capillary sequencer (Applied Biosystems, Foster City, CA, USA) at the Georgia Genomics Facility and scored by eye in Peakscanner v.1.0 (Applied Biosystems) and GeneMarker v.1.8 (Softgenetics LLC, State College, PA, USA).

Linkage groups were generated in both TMAP (Cartwright *et al.*, 2007) and MAPMAKER 3.0 (Lander *et al.*, 1987; Lincoln *et al.*, 1992) with LOD ⩾ 8 and a maximum distance of 40 cM. Marker order was determined in TMAP (Cartwright *et al.*, 2007). Initially unlinked markers were added to the existing linkage groups at a maximum distance of 45 cM and LOD ⩾ 3 using the 'near' command in MAPMAKER 3.0. Total map length was calculated by summing the lengths of the linkage groups. Average marker spacing and map coverage was estimated as in Fishman *et al.* (2001). Genome length was calculated using two methods. First, the genome length was estimated by adding the length of an average marker interval to each end of each linkage group and summing the lengths of the linkage groups. Second, the genome length was estimated as in method 4 of Chakravarti *et al.* (1991). Map coverage was calculated separately for each of these genome length estimates.

Transmission ratio distortion
Regions of transmission ratio distortion (TRD) are potentially important for preventing (or favoring) locus-specific gene flow between *I. nelsonii* and *I. hexagona* when interspecific pollination occurs between the two species. Deviations from expected Mendelian segregation ratios (1AA:2Aa:1aa) in the F_2 generation were analyzed for each microsatellite marker by χ^2 analyses (2 df). For those loci that significantly deviated from 1:2:1 expectations, we further explored for transmission bias (that is, whether *I. nelsonii* or *I. hexagona* homozygotes were overrepresented at each locus), using χ^2 analyses (1 df).

Flower color and morphology
Morphological characters potentially responsible for differential pollinator attraction were measured in the Texas State University greenhouses during the spring of 2009. The total length of the sepal, the length of the sepal blade and sepal stalk, width of the sepal and flower stalk height were measured on the first flower of each plant on the second day when the flower was fully opened.

I. nelsonii and *I. hexagona* flowers differ in multiple aspects of color, with *I. nelsonii* flowers being dark red and *I. hexagona* flowers being blue. The concentration of anthocyanin pigments in a single petal of each flower was estimated based on absorbance (Wilken, 1982). Petals were used instead of sepals as they do not have nectar guides, and color is relatively uniform throughout the entirety of the petal. Anthocyanins were extracted from one pre-weighed petal using acidified methanol (1% w/v HCl in methanol). A subset of individual samples (including red, blue and hybrid flowers) was screened between 400 and 800 nm on a Biomate 3 UV–vis spectrophotometer (Thermo Fisher Scientific, MA, USA). All samples in this subset revealed a maximum absorbance at 537 nm, so absorbance of the full set of samples was measured only at 537 nm. Absorbance values were divided by the weight of the petal to calculate the concentration of anthocyanin pigment (Wilken, 1982). These species also differ with respect to nectar guide area. *I. nelsonii* flowers are

generally devoid of a nectar guide, while *I. hexagona* flowers display a prominent nectar guide on each sepal. The length and width of the nectar guide of the pure species and F_2 plants were both measured in ImageJ (Rasband, 1997–2011). As *Iris* nectar guides are roughly triangular, the area of the nectar guide was calculated as the area of a triangle.

Phenotypic correlations between traits may potentially result from genetic correlation owing to pleiotropy or tight linkage between genes. Phenotypic correlations in the F_2 mapping population were estimated for all pairwise trait combinations. The significance of each phenotypic correlation was assessed after sequentially rejective Bonferroni tests (Holm, 1979).

Quantitative trait locus (QTL) analyses

Genomic regions associated with variation in floral characteristics were detected by composite interval mapping (Zeng, 1994) in Windows QTL Cartographer version 2.5.10 (Wang *et al.*, 2011) using forward and backward regression with the programs default settings (2 cM intervals, 10 cM window size, 5 control markers). A genome-wide significance threshold was set for each trait after 1000 permutations of the data (Churchill and Doerge, 1994; Doerge and Churchill, 1996). A drop below the permutation threshold or a change in the direction of the additive effect was used to distinguish among QTLs on the same linkage group.

RESULTS

Linkage map

All except four markers coalesced into the 22 linkage groups (Figure 1). The remaining markers were unlinked at the minimum criteria set for linking unlinked markers (LOD $\geqslant$ 3, maximum distance 45 cM). For convenience, the linkage groups detected in this mapping population are named to correspond with the linkage groups in Tang *et al.* (2010). These groups corresponded with 20 of the 21 linkage groups detected in reciprocal backcross linkage maps developed for the closely related *I. fulva* and *I. brevicaulis* species (Tang *et al.*, 2010; Supplemental Figure). The linkage map produced by Tang *et al.* (2010) is denser than the current map (average 4.6 cM intervals between markers in Tang *et al.*, 2010 versus the 12.4 cM intervals in this map). The reduced density of the current map is attributed to the fact that the microsatellite markers used in this and the Tang *et al.* (2010) study were developed from *I. brevicaulis* and *I. fulva* individuals and some of these loci did not amplify in the *I. nelsonii* × *I. hexagona* population or were not variable between the mapping parents (IhA32 and In10). As this map contains fewer loci than the map produced by Tang *et al.* (2010), including markers necessary to link distal ends of the linkage groups, some of the larger linkage groups detected by Tang *et al.* (2010) were split into the smaller 'unlinked' linkage groups by the mapping programs with this population. Markers from the ends of the linkage groups 1, 2 and 7, respectively, grouped together (Figure 1), yet because of the large recombination distance between the ends of these linkage groups, they did not link together in the current map. As such, the portions of the current linkage groups are labeled with 'a' and 'b' in Figure 1. As the markers from the 'a' and 'b' segments are not linked, the orientation of the segments in relation to each other cannot be determined. The placement of the segments in Figure 1 is one interpretation of the possible placement of these segments. No markers from the relatively small linkage group 20 from Tang *et al.* (2010) were amplified in this F_2 population. The sum length of this *I. nelsonii* × *I. hexagona* linkage map was 1379.9 cM, with an average marker spacing of 12.4 cM. The estimated genome length was calculated two ways, which yielded similar results. If calculated by adding twice the marker interval spacing to each linkage group, the genome length was estimated as 1926.9 cM. If calculated as method 4 from Chakravarti *et al.* (1991), the genome length was estimated as 1948.8 cM. Each estimate of genome length was used

in calculations of genome coverage. Based on these calculations, $\sim$ 74% of the genome is within 10 cM of a marker.
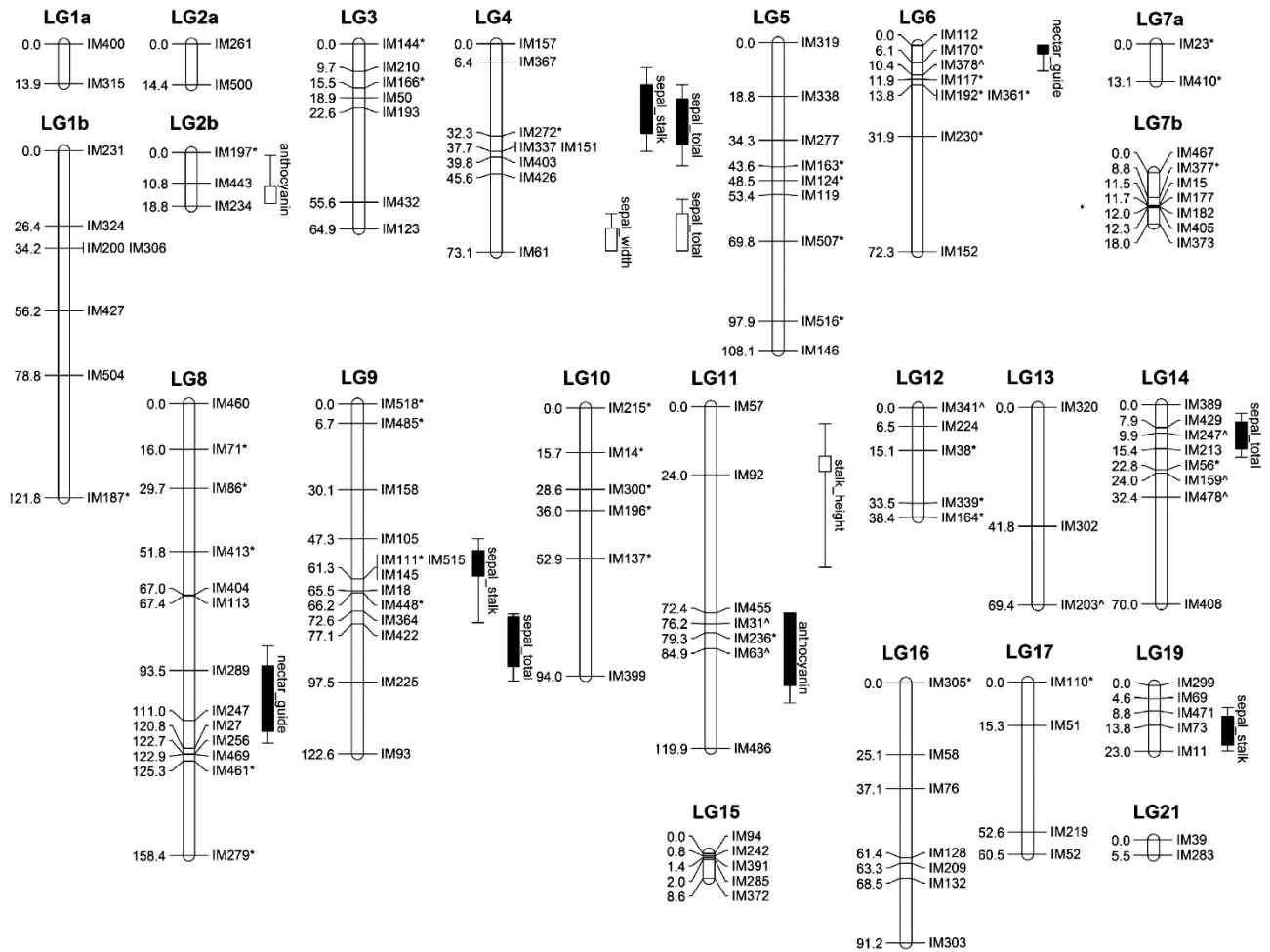
Transmission ratio distortion

TRD was observed for approximately one-third of the marker loci (Figure 2). Some markers were difficult to genotype with certainty. These markers were re-coded to reflect that uncertainty, which results in a potential loss of genetic information, (for example, for some individuals, it was difficult to distinguish with certainty among homozygotes and heterozygotes for the *I. nelsonii* allele (to use an example)—yet it was clear that the individual was not homozygous for the *I. hexagona* allele. These individuals were all coded as a separate category (essentially as '*not homozygous for I. hexagona*') recognized by the mapping programs). Segregation at these loci was investigated under the simplifying assumption that approximately half of the re-coded loci were homozygotes and half were heterozygotes. If this investigation resulted in a substantial change in the TRD (and *P*-value), the marker was designated with a caret ($\wedge$) on the linkage map and TRD figures (Figures 1 and 2). No directional bias in TRD was observed. Of the markers that revealed significant TRD and uncertain genotypes did not affect the interpretation of the results, homozygotes for the *I. nelsonii* allele were overrepresented for 13 markers, while homozygotes for the *I. hexagona* allele were over-represented in 14 markers. For the remaining markers, heterozygotes were largely underrepresented (10/13 markers had a heterozygote deficiency, Figure 2).

Flower color and morphology

A majority of the F_2 plants ($N = 184$) flowered during the 2009 flowering season. However, only six pure-species *I. hexagona* and five *I. nelsonii* individuals flowered in the experimental setup during the 2009 flowering season. Owing to this reduced sample size of pure-species individuals and lack of information from the mapping parents, QTL effect sizes are only reported as a proportion of the variance explained in the F_2 population. The morphological measurements made in the greenhouse (Tables 1 and 2) reflected measurements made in natural populations by Randolph (1966), suggesting that the few pure-species plants that did flower in the greenhouse represent typical samples of the species. The flower stalks of the *I. nelsonii* individuals ($\mu = 51.4 \pm 12.14$ cm) were slightly shorter than those of *I. hexagona* ($\mu = 64.5 \pm 11.77$ cm; $t = 1.6$, df = 7, $P = 0.15$). One QTL was detected that explained a small percentage of the variance in the F_2 population (proportion of the variance explained = 0.09; Figure 1, Table 2). At this QTL, the *I. hexagona* allele resulted in a decrease in flower stalk height.

In *Iris* flowers, the sepal subtends the anther and stigma and is thus likely important in pollinator attraction. The sepal shape of *I. nelsonii* and *I. hexagona* differ in that the sepals of *I. nelsonii* are reflexed and *I. hexagona* sepals are upright. As the *I. nelsonii* sepal is reflexed, the sepal stalk of the *I. nelsonii* flowers ($\mu = 1.84 \pm 0.36$ cm) is significantly shorter than that of the *I. hexagona* flowers ($\mu = 3.67 \pm 0.45$ cm; $t = 6.6$, df = 7, $P = 0.0003$). Three QTLs were detected for sepal stalk length. The *I. hexagona* allele results in an increase in the sepal stalk length at all QTLs detected. The sepal blade of *I. nelsonii* individuals ($\mu = 4.85 \pm 0.60$ cm) in the greenhouse was also significantly shorter than the sepal blade of *I. hexagona* individuals ($\mu = 6.25 \pm 0.51$ cm; $t = 3.8$, df = 7, $P = 0.007$). No QTLs were detected for sepal blade length. The total length of sepals was significantly lower in *I. nelsonii* ($\mu = 6.69 \pm 0.29$ cm) than in *I. hexagona* ($\mu = 9.92 \pm 0.82$ cm; $t = 7.5$, df = 7, $P = 0.0001$). Three of the four QTLs detected for sepal total length were in the expected direction, where the *I. hexagona* allele

Figure 1 Linkage map created from an F$_2$ cross between *I. nelsonii* and *I. hexagona*. The names of both the markers and linkage groups reflect those used by Tang *et al.* (2010). Markers revealing significant transmission ratio distortion are denoted with an asterisk after the marker name. Markers with a large number of uncertain genotypes that substantially influenced conclusions about distortion are designated with a caret (^). Boxes indicate the 1-LOD confidence interval and lines indicate the 2-LOD confidence interval for Quantitative trait loci (QTLs) associated with variation in phenotypic traits. Filled boxes indicate QTLs at which the *I. hexagona* allele increased the trait value. Open boxes indicate QTLs at which the *I. hexagona* allele decreased the trait value.

results in an increase in sepal total length. The *I. hexagona* allele decreases the trait value for the other QTL. The sepal width of *I. nelsonii* flowers ($\mu = 3.27 \pm 0.34$ cm) was also smaller than *I. hexagona* flowers ($\mu = 4.13 \pm 0.47$ cm; $t = 2.9$, df $= 5$, $P = 0.04$). One QTL was detected for sepal width (Figure 1; Table 2). At this QTL, the *I. hexagona* allele decreases the trait mean, which is opposite expectations given the species means.

Many of the sepal measurements were correlated (Table 1). In two cases, this correlation was coupled with overlapping QTLs. The total sepal length and the sepal stalk length are strongly correlated and have overlapping QTLs on LG4 with effects in the same direction (Figure 1; Table 2). Sepal width and total sepal length are also correlated and QTLs detected on LG4 were overlapping and had effects in the same direction (Figure 1; Table 2).

The species also differ in color, where *I. nelsonii* flowers are red, as is typical for many hummingbird pollinated flowers, and *I. hexagona* flowers are blue—typical of many bee-pollinated flowers. *I. nelsonii* flowers contained a higher concentration of anthocyanin pigments ($\mu = 0.013 \pm 0.001$ OD per mg) than did *I. hexagona* flowers ($\mu = 0.005 \pm 0.0007$ OD per mg; $t = 10.4$, df $= 8$, $P < 0.0001$). Two QTLs were detected that had mixed effects on anthocyanin

concentration (Figure 1; Table 2). Also, *I. nelsonii* typically has no, or a very small, nectar guide ($\mu = 0.06 \pm 0.06$ cm) while the nectar guide on *I. hexagona* ($\mu = 0.64 \pm 0.15$ cm) is prominent ($t = 7.0$, df $= 9$, $P < 0.0001$). Two QTLs were detected that were associated with variation in nectar guide. As predicted by the species mean difference, the *I. hexagona* allele increased the trait mean at both QTLs.

DISCUSSION
Genomic collinearity
In order for new homoploid hybrid species to arise and persist, they must evolve reproductive isolation from their progenitor species at a relatively early stage. Early verbal models of homoploid hybrid speciation invoked chromosomal rearrangements and the resulting infertility of F$_1$ hybrids as the most likely mechanism by which new homoploid species arise (Grant, 1971). Computer simulations have revealed that, although chromosomal rearrangements have an important role in the establishment of homoploid hybrid species, ecological isolation can greatly increase the degree to which these newly derived species are maintained over time (Buerkle *et al.*, 2000). Indeed, studies in *Helianthus* support chromosomal differences coupled with ecological isolation as a primary mechanism by which repeated homoploid
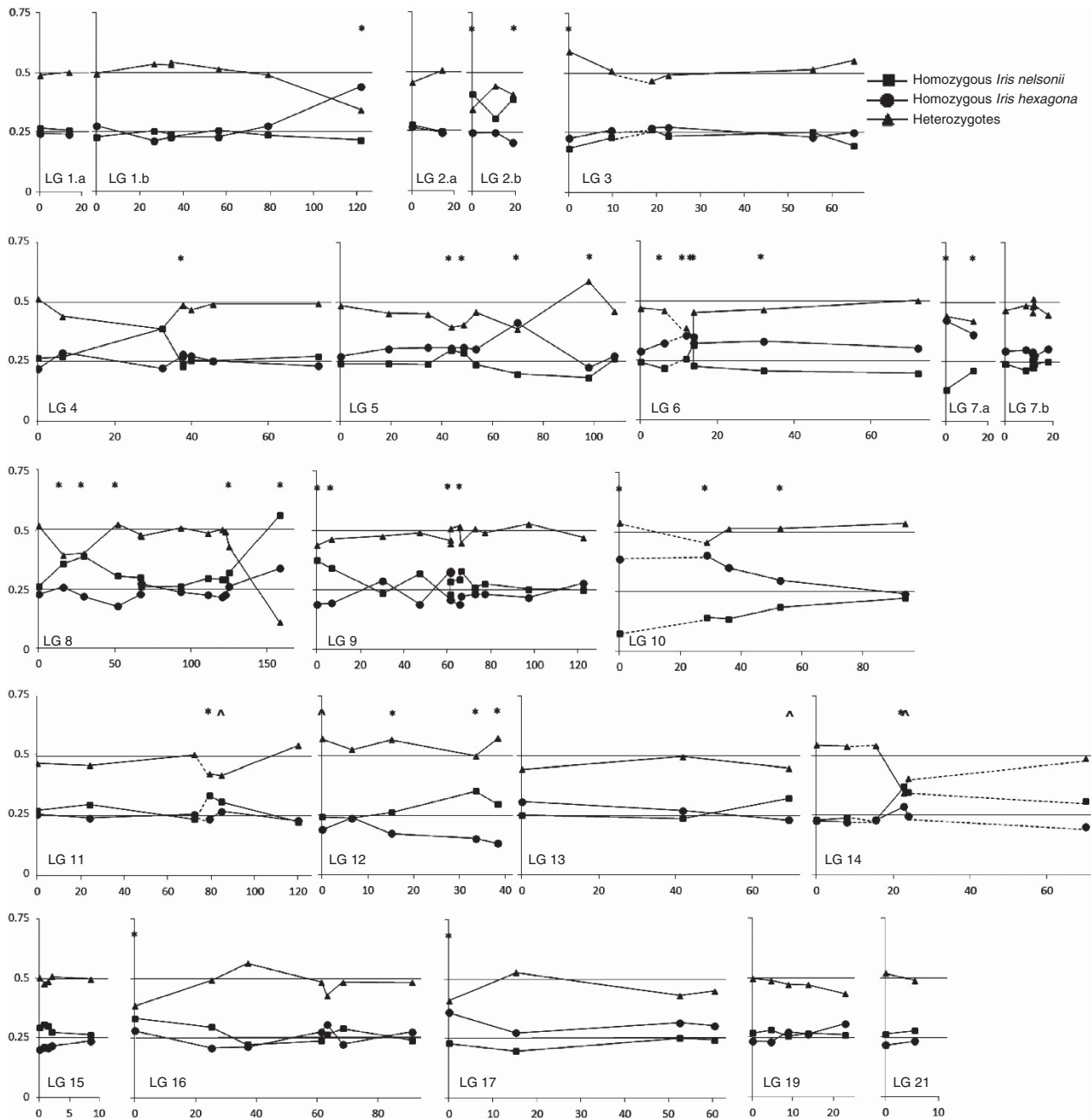
Figure 2 Observed genotype frequencies of homozygous *I. nelsonii* (squares), homozygous *I. hexagona* (circles) and heterozygotes (triangles). The X-axis denotes the distances (cM) along each linkage group. Lines at 0.25 and 0.5 represent Mendelian expected frequencies for homozygotes and heterozygotes, respectively. Markers that deviated from these expectations ($P < 0.05$) are designated with an asterisk (*). Genotype frequencies of markers designated with a caret (^) are not represented because these markers had a large number of undistinguishable genotypes.

hybrid species have arisen (Rieseberg *et al.*, 1995, 2003; Lai *et al.*, 2005). However, hybrid speciation may also be achieved without chromosomal rearrangements if genic incompatibilities and/or ecological divergence isolate the hybrid species from its progenitors (Templeton, 1981; Jiggins *et al.*, 2008). The relative importance of karyotypic differences versus genic incompatibilities is not known because there are relatively few studies specifically examining the genomic collinearity of homoploid hybrid species and their progenitors (but see Rieseberg *et al.*, 1995; Lai *et al.*, 2005). While studies in *Helianthus* support chromosomal differences as a largely important barrier to

gene flow (Rieseberg *et al.*, 1995; Lai *et al.*, 2005), a recent study in *Cottus* (Stemshorn *et al.*, 2011) and the current study reveal high degrees of genomic collinearity between the homoploid hybrid lineage and the progenitors, suggesting that other mechanisms are potentially responsible for reproductive isolation between the hybrid lineage and progenitors.

The genomes of all four hybridizing Louisiana Iris species show a high degree of genetic collinearity. Although *I. hexagona* has a different chromosome number than the other three species, interspecific linkage maps between the species reveal little evidence of

Table 1 Spearman's correlation coefficients for tests of pairwise phenotypic correlations

	Stalk height	Sepal stalk	Sepal blade	Sepal total	Sepal width	Nectar guide	Anthocyanin
Stalk height	170						
Sepal stalk	0.05	176					
Sepal blade	0.08	**0.34**	174				
Sepal total	0.06	**0.66**	**0.92**	176			
Sepal width	0.11	0.13	**0.49**	**0.43**	175		
Nectar guide	0.06	0.15	*0.23*	**0.25**	**0.24**	168	
Anthocyanin	−0.17	−0.18	*−0.23*	*−0.27*	**−0.35**	−0.02	115

Coefficients in bold are significant after a sequentially rejective Bonferroni test. Italicized coefficients were significant before, but not after, correction with the sequentially rejective Bonferroni test. Sample size for each trait is given in the diagonal.

Table 2 F2 means, sample sizes, and QTL associated with variation in floral characteristics in *Iris nelsonii* × *I. hexagona* F2 hybrids

Trait	N	F_2 mean (s.d.)	Linkage group	Location (cM)	Proportion of the variance explained	Additive effect	Dominance effect
Stalk height (cm)	170	87.63 (13.96)	LG14	21.4 (6.0–56.4)	0.09	−3.228	7.414
Sepal stalk (cm)	176	3.14 (34)	LG4	21.4 (8.4–37.7)	0.16	0.183	0.013
Sepal stalk (cm)	176	3.14 (34)	LG9	56.3 (47.3–76.6)	0.10	0.130	0.114
Sepal stalk (cm)	176	3.14 (34)	LG19	13.8 (7.6–22.8)	0.09	0.136	0.052
Sepal blade (cm)	174	5.81 (59)	no QTL detected				
Sepal total (cm)	176	8.95 (77)	LG4	28.4 (14.4–42.8)	0.12	0.367	0.042
Sepal total (cm)	176	8.95 (77)	LG4	72.6 (54.6–72.6)	0.09	−0.338	−0.033
Sepal total (cm)	176	8.95 (77)	LG9	83.1 (73.6–97.1)	0.10	0.303	0.178
Sepal total (cm)	176	8.95 (77)	LG14	0.0991 (0.03–18)	0.14	0.389	−0.279
Sepal width (cm)	175	4.32 (39)	LG4	72.6 (59.6–72.6)	0.12	−0.189	−0.075
Nectar guide area (cm^2)	168	0.61 (47)	LG6	0 (0–9.1)	0.14	0.245	−0.049
Nectar guide area (cm^2)	168	0.61 (47)	LG11	104.9 (84.9–118.9)	0.21	0.307	0.046
Anthocyanin (OD per mg)	115	0.011 (0026)	LG2B	17.8 (1–17.8)	0.13	−0.001	−0.001
Anthocyanin (OD per mg)	115	0.011 (0026)	LG11	82.3 (72.4–103.9)	0.24	0.002	0.001

The location of the highest likelihood ratio is given with 2-logarithm of odds confidence intervals in parentheses. The magnitude of QTL effect is reported as the proportion of the variance explained in the mapping population. Additive and dominance effects are in units of the trait.

major chromosomal rearrangements between it and the other three Louisiana Iris species (Tang *et al.*, 2010; E. Ballerini *et al.*, unpublished data). The markers in the current study grouped as in maps produced by Tang *et al.* (2010), and updated by E. Ballerini *et al.*, unpublished data), from crosses between *I. brevicaulis* and *I. fulva*, with few exceptions. Marker IM192 is the terminal marker of LG 6 in the *I. brevicaulis* × *I. fulva* map, but is 13.8 cM from the top in the current map. Also, on LG9, marker spacing in the current map is greater than marker spacing in Tang *et al.* (2010) and marker IM364 is the terminal marker of LG 9 in Tang *et al.* (2010) but in the middle (72.6 cM) of LG 9 in the current map (Figure 1; Supplementary Figure). Future mapping studies in a cross between *I. nelsonii* and *I. fulva* and between *I. hexagona* and *I. fulva* will allow us to identify the specific order of markers within each of the species. However, the high degree of genetic collinearity observed between these interspecific maps, combined with the fact that F₁ hybrids do not reveal substantial reductions in pollen fertility (*I. fulva* × *I. nelsonii*, *I. nelsonii* × *I. fulva*, and *I. nelsonii* × *I. hexagona* preliminary data shows F₁ fertility is ~85% that of pure species fertility) imply that major chromosomal rearrangements are not effecting a high degree of postzygotic isolation, lending support to Randolph's (1966) hypothesis of ecological isolation being primarily responsible for the origin and maintenance of *I. nelsonii* in its unique cypress swamp habitat.

Transmission ratio distortion

Non-Mendelian transmission of alleles is routinely reported across a wide variety of interspecific and intraspecific crosses and across a wide variety of taxa (Fishman *et al.*, 2001; Bouck *et al.*, 2005; Hall and Willis, 2005; Tang *et al.*, 2010; Casellas *et al.*, 2012; Koevoets *et al.*, 2012). TRD may result from any number of post-pollination prezygotic (for example Fishman *et al.*, 2008), or postzygotic (prior to genotyping) biological processes. Our crossing design could have resulted in some amount of inbreeding depression, as the original parents were wild-collected and they could have been harboring some deleterious alleles in heterozygous form. This could result in an underrepresentation of parental genotypes linked to those deleterious alleles or an overrepresentation of heterozygotes. As such, the TRD observed for loci in which either *I. nelsonii* or *I. hexagona* homozygotes are underrepresented could be caused by post-pollination barriers and/or postzygotic processes (including inbreeding depression).

However, for the 13 markers in which TRD was found and the parental genotypes were roughly equal, ten markers revealed heterozygote deficiencies. This pattern cannot be explained by inbreeding depression, and suggests selection against heterozygote individuals at those loci. In reciprocal backcross linkage mapping populations produced between *I. fulva* and *I. brevicaulis* and germinated, and grown as seedlings in the same greenhouse as the *I. nelsonii* × *I. hexagona*

mapping population roughly one-third of the markers revealed significant TRD (Bouck *et al.*, 2005; Tang *et al.*, 2010). In those same maps, TRD was largely asymmetric, in that *I. fulva* alleles were overrepresented in each genetic background (Tang *et al.*, 2010). Indeed, introgression in natural hybrid populations between these species often shows a pattern of asymmetric introgression of *I. fulva* alleles across species boundaries (Arnold and Martin, 2010). However, markers in the current F$_2$ mapping population showed no such asymmetries.

Genetic architecture of floral characteristics

Ecological divergence is important in reducing gene flow between the homoploid hybrid lineage and its progenitors (Buerkle *et al.*, 2000; Gross and Rieseberg, 2005). *I. nelsonii* is likely isolated from at least two of its progenitors (*I. hexagona* and *I. brevicaulis*) by pollinator isolation and differs from all of its progenitors in its unique suite of floral characteristics (Randolph, 1966). As a result of these highly divergent floral morphologies, *I. nelsonii* and *I. hexagona* are primarily visited by different pollinator groups. *I. hexagona* is primarily pollinated by bumblebees (Emms and Arnold, 2000) while *I. nelsonii* is primarily pollinated by hummingbirds (Taylor *et al.*, 2012).

The unique floral morphology of *I. nelsonii* is likely due to inheritance of a mixture of loci from the progenitor species. As such, *I. nelsonii* shares some floral characteristics with *I. fulva* and others with *I. hexagona*, but it also has characteristics that are outside of the means of the other species (Randolph, 1966). Here, we used QTL mapping to identify loci that differentiate *I. nelsonii* from one of its progenitor species, *I. hexagona*. These loci serve as hypotheses for loci under selection during the formation of *I. nelsonii*. These loci are also likely responsible for maintaining species barriers via pollinator isolation where these species occur in sympatry. Divergent floral morphologies may directly cause reduced interspecific visitation between these two taxa as has been observed between *I. fulva* and *I. brevicaulis* (Martin *et al.*, 2008) and between *I. fulva* and *I. hexagona* (Emms and Arnold, 2000).

QTL mapping studies have often found genomic regions that influence variation in multiple floral traits (for example, Juenger *et al.*, 2000; Fishman *et al.*, 2002; Goodwillie *et al.*, 2006; Bouck *et al.*, 2007). Pleiotropy or tight linkage of QTLs that influence floral traits may constrain floral evolution in a hybrid zone. We detected some colocalization of QTLs for traits in this mapping population. QTLs for sepal traits colocalized on LG4 and LG9. These overlapping QTLs influenced traits for which we detected positive phenotypic correlations (Table 1). Although the remainder of the significant phenotypic correlations is not explained by colocalized QTLs in this map, we caution that many QTLs, especially those of small effect, may remain undetected due to small sample size, as at least half of the phenotypic variance in the F$_2$ population remains unexplained for all traits.

The genetic architecture of floral characteristics in this system is similar to studies examining the genetic architecture of floral characteristics in other species. Here, we detected two QTLs for anthocyanin concentration that together explained a large portion of the variance in the F$_2$ population (total ∼37%; Table 2). While QTL mapping studies, especially those with limited sample sizes, may tend to overestimate effect sizes (Beavis, 1998), a number of other studies that have quantified flower color in mapping populations have generally detected few loci of large effect on the trait as well (for example, Bradshaw *et al.*, 1995; Bouck *et al.*, 2007; reviewed in Galliot *et al.*, 2006). We also detected two QTLs for nectar guide area that explained ∼35% of the variation in the trait (Table 2), which is similar to the findings of Bouck *et al.* (2007) in a cross between the

other two Louisiana Iris species (*I. brevicaulis* and *I. fulva*). In contrast to floral color differences between species, differences in other aspects of floral morphology appear to be influenced by a larger number of minor QTLs (Fishman *et al.*, 2002; Bouck *et al.*, 2007; Kim and Rieseberg, 1999; reviewed in Galliot *et al.*, 2006; but see Bradshaw *et al.*, 1995). Here, we similarly detected between 0 and 4 QTLs for each morphological trait, with an average of 0.11 ± 0.03 proportion of the variance explained by each of these loci.

The large effect of the color loci and the relatively small effect of the morphological loci suggest that the color difference between species may be accomplished with relatively few substitutions, while more mutational steps lay between the divergent morphologies of closely related species (reviewed in Galliot *et al.*, 2006). Understanding the genetic architecture of floral traits and pollinator visitation allows an investigation of the loci that are under selection by pollinators (for example, Bradshaw and Schemske, 2003). The genetic architecture of floral differences and the effect of these differences on pollinator visitation have been studied in few systems. In *Mimulus* and *Petunia*, mutations with large effect on color (carotenoids and anthocyanins, respectively) also have a large effect on pollinator visitation (Bradshaw and Schemske, 2003; Hoballah *et al.*, 2007). In analyses of pollinator visitation in experimental arrays of Louisiana Iris, pollinator preference QTLs overlapped with brightness and hue QTLs of relatively small effect in a backcross population between *Iris fulva* and *I. brevicaulis* (Martin *et al.*, 2008). The current mapping population has an advantage over the *I. brevicaulis* × *I. fulva* mapping population for examining pollinator preferences, because *I. nelsonii* and *I. hexagona* have near-identical flowering phenologies. *Iris fulva* and *I. brevicaulis* have highly divergent flowering times (the peak flowering times of these species are shifted by approximately a month; Martin *et al.*, 2007), which potentially results in experimental arrays that are offered to the pollinators differing throughout the field season, or the 'training' of pollinators to prefer certain floral traits over time.

Summary and conclusions

We have shown that *I. nelsonii*, a homoploid hybrid, has a genome that is highly collinear with its progenitor species, which comports with the relatively high fertility observed when F$_1$ hybrids are produced between *I. nelsonii* and its parents. This suggests that barriers other than karyotypic rearrangements were largely responsible for the early establishment of this species. Indeed, Randolph (1966) posited that ecological barriers were likely important in reducing gene flow between *I. nelsonii* and its progenitors, and Taylor *et al.* (2011) have shown that, in fact this hybrid taxon responds differently to abiotic environmental factors than its parental species. This mapping population and the newly-created map presented here will enable us to examine the genetic architecture of ecological divergence between *I. nelsonii* and *I. hexagona*. Pollinator isolation is a potentially strong ecological barrier between *I. nelsonii* and *I. hexagona,* and we are now in the position to perform pollinator array experiments to examine the genetic architecture of pollinator isolation between these species, and to determine whether the genetic architecture of the floral traits examined here reflects that of pollinator isolation.

DATA ARCHIVING

Genotype and phenotype data have been deposited at Dryad (doi:10.5061/dryad.6cn04).

CONFLICT OF INTEREST

The authors declare no conflict of interest.

ACKNOWLEDGEMENTS

Arnold ML (1993). *Iris nelsonii* (Iridaceae): origin and genetic composition of a homoploid hybrid species. *Am J Bot* **80**: 577–583.

Arnold ML, Hamrick JL, Bennett BD (1990). Allozyme variation in Louisiana irises: a test for introgression and hybrid speciation. *Heredity* **65**: 297–306.

Arnold ML, Martin NH (2010). Hybrid fitness across time and habitats. *Trends in Ecology and Evolution* **25**: 530–536.

Beavis W (1998). QTL analyses: power, precision, and accuracy. In: Paterson AH (ed) *Molecular Dissection of Complex Traits*. CRC Press: Boca Raton, pp 145–162.

Bennett BD, Grace JB (1990). Shade tolerance and its effect on the segregation of two species of Louisiana Iris and their hybrids. *Am J Bot* **77**: 100–107.

Bouck A, Peeler R, Arnold ML, Wessler SR (2005). Genetic mapping of species boundaries in Louisiana irises using IRRE retrotransposon display markers. *Genetics* **171**: 1289–1303.

Bouck A, Wessler SR, Arnold ML (2007). QTL analysis of floral traits in Louisiana Iris hybrids. *Evolution* **61**: 2308–2319.

Bradshaw Jr HD, Schemske DW (2003). Allele substitution at a flower colour locus produces a pollinator shift I monkeyflowers. *Nature* **426**: 176–178.

Bradshaw Jr HD, Wilbert SM, Otto KG, Schemske DW (1995). Genetic mapping of floral traits associated with reproductive isolation in monkeyflowers (*Mimulus*). *Nature* **376**: 762–765.

Buerkle CA, Morris RJ, Asmussen MA, Rieseberg LH (2000). The likelihood of homoploid hybrid speciation. *Heredity* **84**: 441–451.

Buerkle CA, Rieseberg LH (2008). The rate of genome stabilization in homoploid hybrid species. *Evolution* **62**: 266–275.

Cartwright DA, Troggio M, Velasco R, Gutin A (2007). Genetic mapping in the presence of genotyping errors. *Genetics* **176**: 2521–2527.

Casellas J, Gularte RJ, Farber CR, Varona L, Mehrabian M, Schadt EE *et al*. (2012). Genome scans for transmission ratio distortion regions in mice. *Genetics* **191**: 247–259.

Chakravarti A, Lasher LK, Reefer JE (1991). A maximum likelihood method for estimating genome length using genetic linkage data. *Genetics* **128**: 175–182.

Churchill GA, Doerge RW (1994). Empirical threshold values for quantiatitve trait mapping. *Genetics* **138**: 963–971.

Coyne JA, Orr HA (1989). Patterns of speciation in Drosophila. *Evolution* **43**: 362–381.

Coyne JA, Orr HA (1997). 'Patterns of speciation in Drosophila' revisited. *Evolution* **51**: 295–303.

Coyne JA, Orr HA (2004). *Speciation*. Sinauer: Sunderland, MA.

Doerge RW, Churchill GA (1996). Permutation tests for multiple loci affecting a quantitative character. *Genetics* **142**: 285–294.

Don RH, Cox PT, Wainwright BJ, Baker K, Mattick J (1991). 'Touchdown' PCR to circumvent spurious priming during gene amplification. *Nucleic Acids Res* **19**: 4008.

Emms SK, Arnold ML (2000). Site-to-site differences in pollinator visitation patterns in a Louisiana iris hybrid zone. *Oikos* **91**: 568–578.

Fishman L, Aagaard J, Tuthill JC (2008). Toward the evolutionary genomics of gametophytic divergence: patterns of transmission ratio distortion in monkeyflower (*Mimulus*) hybrids reveal a complex genetic basis for conspecific pollen precedence. *Evolution* **62**: 2958–2970.

Fishman L, Kelly AJ, Morgan E, Willis JH (2001). A genetic map in the *Mimulus guttatus* species complex reveals transmission ratio distortion due to heterospecific interactions. *Genetics* **159**: 1701–1716.

Fishman L, Kelly AJ, Willis JH (2002). Minor quantitative trait loci underlie floral traits associated with mating system divergence in *Mimulus*. *Evolution* **56**: 2138–2155.

Galliot C, Stuurman J, Kuhlemeier C (2006). The genetic dissection of floral pollination syndromes. *Curr Opin Plant Biol* **9**: 78–82.

Goodwillie C, Ritland C, Ritland K (2006). The genetic basis of floral traits associated with mating system evolution in *Leptosiphon* (Polemoniaceae): an analysis of quantitative trait loci. *Evolution* **60**: 491–504.

Grant V (1971). *Plant Speciation*. Columbia University Press: New York.

Gross BL, Rieseberg LH (2005). The ecological genetics of homoploid hybrid speciation. *J Hered* **96**: 241–252.

Hall MC, Willis JH (2005). Transmission ratio distortion in intraspecific hybrids of *Mimulus guttatus*. *Genetics* **170**: 375–386.

Hoballah ME, Gubitz T, Stuurman J, Broger L, Barone M, Mandel T *et al*. (2007). Single gene-mediated shift in pollinator attraction in *Petunia*. *Plant Cell* **19**: 779–790.

Holm S (1979). A simple sequentially rejective multiple test procedure. *Scan J Statist* **6**: 65–70.

James JK, Abbott RJ (2005). Recent, allopatric, homoploid hybrid speciation: the origin of *Senecio squalidus* (Asteraceae) in the British Isles from a hybrid zone on Mount Etna, Sicily. *Evolution* **59**: 2533–2547.

Jiggins CD, Salazar C, Linares M, Mavarez J (2008). Hybrid trait speciation and *Heliconius* butterflies. *Phil Trans R Soc B* **363**: 3047–3054.

Juenger T, Purugganan M, Mackay TFC (2000). Quantitative trait loci for floral morphology in *Arabidopsis thaliana*. *Genetics* **156**: 1379–1392.

Karrenberg S, Lexer C, Rieseberg L (2007). Reconstructing the history of selection during homoploid hybrid speciation. *Amer Nat* **169**: 725–737.

Kim S-C, Rieseberg LH (1999). Genetic architecture of species differences in annual sunflowers: implications for adaptive trait introgression. *Genetics* **153**: 965–977.

Koevoets T, Niehuis O, van de Zande L, Beukeboom LW (2012). Hybrid incompatibilities in the parasitic wasp genus *Nasonia*: negative effects of hemizygosity and the identification of transmission ratio distortion loci. *Heredity* **108**: 302–311.

Lai Z, Nakazato T, Salmaso M, Burke JM, Tang S, Knap SJ *et al*. (2005). Extensive chromosomal repatterning and the evolution of sterility barriers in hybrid sunflower species. *Genetics* **171**: 291–303.

Lander ES, Green P, Abrahamson J, Barlow A, Daly MJ, Lincoln SE *et al*. (1987). MAPMAKER: an interactive computer package for constructing primary genetic linkage maps of experimental and natural populations. *Genomics* **1**: 174–181.

Lincoln SE, Daly MJ, Lander ES (1992). *Constructing Genetic Maps with MAPMAKER/ EXP 3.0 Manual*. Whitehead Institute: Cambridge, MA.

Mallett J (2007). Hybrid speciation. *Nature* **446**: 279–283.

Malone JH, Fontenot BE (2008). Patterns of reproductive isolation in toads. *PLoS ONE* **3**: e3900.

Martin NH, Bouck AC, Arnold ML (2007). The genetic architecture of reproductive isolation in Louisiana irises: flowering phenology. *Genetics* **175**: 1803–1812.

Martin NH, Sapir Y, Arnold ML (2008). The genetic architecture of reproductive isolation in Louisiana irises: pollination syndromes and pollinator preferences. *Evolution* **62**: 740–752.

Moyle LC, Olson MS, Tiffin P (2004). Patterns of reproductive isolation in three angiosperm genera. *Evolution* **58**: 1195–1208.

Randolph LF (1966). Iris nelsonii, a new species of Louisiana Iris of hybrid origin. *Baileya* **14**: 143–169.

Randolph LF, Mitra J, Nelson IS (1961). Cytotaxonomic studies of Louisiana Irises. *Bot Gazette* **123**: 125–133.

Rasband WS (1997–2011). *ImageJ*. U. S. National Institutes of Health: Bethesda, Maryland, USA. http://imagej.nih.gov/ij/.

Rieseberg (2000). Crossing relationships among ancient and experimental sunflower hybrid lineges. *Evolution* **54**: 859–865.

Rieseberg LH, Raymond O, Rosenthal DM, Lai Z, Livingstone K, Nakazato T *et al*. (2003). Major ecological transitions in wild sunflowers facilitated by hybridization. *Science* **301**: 1211–1216.

Rieseberg LH, Van Fossen C, Desrochers AM (1995). Hybrid speciation accompanied by genomic reorganization in wild sunflowers. *Nature* **375**: 313–316.

Rieseberg LH, Willis JH (2007). Plant speciation. *Science* **317**: 910–914.

Salazar C, Baxter SW, Pardo-Diaz C, Wu G, Surridge A, Linares M *et al*. (2010). Genetic evidence for hybrid trait speciation in *Heliconius* butterflies. *PLoS Genet* **6**: e1000930.

Scopece G, Widmer A, Cozzolino S (2008). Evolution of postzygotic reproductive isolation in a guild of deceptive orchids. *Amer Nat* **171**: 315–326.

Stemshorn KC, Reed FA, Nolte AW, Tautz D (2011). Rapid formation of distinct hybrid lineages after secondary contact of two fish species (Cottus sp.). *Mol Ecol* **20**: 1475–1491.

Tang S, Okashah RA, Cordonnier-Pratt MM, Pratt LH, Johnson VE, Taylor CA *et al*. (2009). EST and EST-SSR marker resources for Iris. *BMC Plant Biol* **9**: 72.

Tang S, Okashah RA, Knapp SJ, Arnold ML, Martin NH (2010). Transmission ratio distortion results in asymmetric introgression in Louisiana Iris. *BMC Plant Biol* **10**: 48.

Taylor SJ, AuBuchon KJ, Martin NH (2012). Identification of Floral Visitors of *Iris nelsonii*. *Southeastern Naturalist* **11**: 141–144.

Taylor SJ, Willard RW, Shaw JP, Dobson MC, Martin NH (2011). Differential response of the homoploid hybrid species *Iris nelsonii* (Iridaceae) and its progenitors to abiotic habitat conditions. *Am J Bot* **98**: 1309–1316.

Templeton AR (1981). Mechanisms of speciation - a population genetic approach. *Ann Rev Ecol Syst* **12**: 23–48.

Wang S, Basten CJ, Zeng Z-B (2011). *Windows QTL Cartographer 2.5*. Department of Statistics, North Carolina State University: Raleigh, NC (http://statgen.ncsu.edu/qtlcart/WQTLCart.htm).

Wilken DH (1982). A simple method for estimating anthocyanin concentrations in tissue extracts. *Phytochemical Bulletin* **15**: 7–13.

Zeng Z-B (1994). Precision mapping of quantitative trait loci. *Genetics* **136**: 1457–1468.

Supplementary Information accompanies the paper on Heredity website (http://www.nature.com/hdy)